Rock Mech. Rock Engng. (2003) 36 (3), 183–208
DOI 10.1007/s00603-002-0042-0

**Rock Mechanics and Rock Engineering**
Printed in Austria

# Open Stope Stability Using 3D Joint Networks

By

**M. Grenon**[1] and **J. Hadjigeorgiou**[2]

[1] Brunswick Mine, Noranda Inc. Bathurst, Canada
[2] Department of Mining, Metallurgical and Materials Engineering, Université Laval, Quebec City, Canada

Received February 23, 2001; accepted October 11, 2002;
Published online January 21, 2003 

## Summary

The most popular exploitation method used in Canadian hard rock mines is open stope mining. Geomechanical design of open stopes relies on a range of analytical, numerical and empirical tools. This paper presents an engineering approach for the analysis and the design of reinforcement for open stopes in jointed rock. The proposed methodology, illustrated by three case studies, relies on developing 3D joint network models from field data. The 3D joint networks have been successfully linked to a 3D limit equilibrium software package. The models account for the finite length of joints as well as the influence of random joints. The integrated approach facilitates comparative analyses of different reinforcement strategies under different degrees of jointing in the hard rock environment.

*Keywords:* Open stope, discontinuity networks, Stability analysis.

## 1. Introduction

The most popular exploitation method in Canadian hard rock mines is open stope mining. The method is best suited to relatively steep dipping, competent ore bodies, surrounded by good quality rock. Ore is produced by drilling and blasting long holes between two sub-levels and is subsequently mucked on the lower sub-level (Fig. 1). Potvin and Hudyma (2000) report that the majority of operations that employ open stope mining favor the use of relatively short, single lift stopes, with fast turnaround times. A short lift implies that the stope height is less than 30 m. A single lift suggests that the stope was excavated between two consecutive levels. The time necessary for preparing a short single lift stope is considerably smaller than for a large open stope. However, a consequence of using short lift stopes is the need for systematic support for the stope roof or back. There are two variations of open stope mining that have received considerable attention. In low

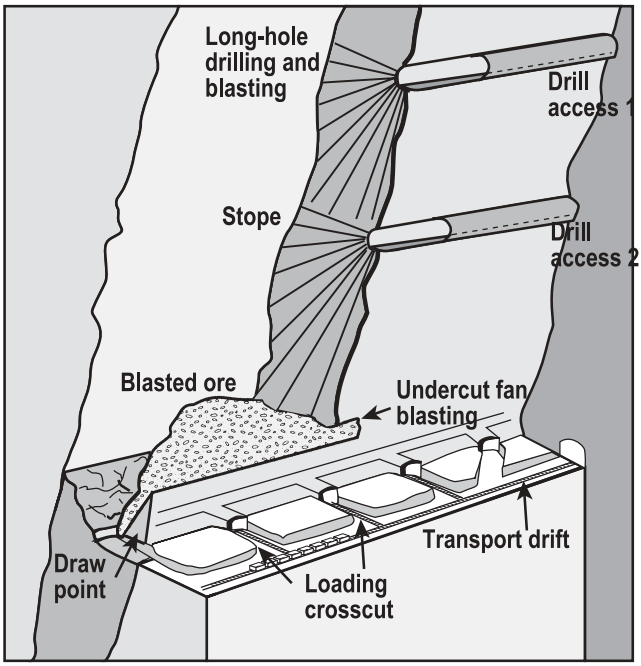


**Fig. 1.** Schematic representation of an open stope, after Hamrin (2001)

stress mining transverse blasthole open stoping is favored as it allows for complex stope sequencing. Referring to Fig. 2, a distinction is made between primary and secondary stopes. Primary stopes are the first to be mined, and if required are then backfilled. Once the majority of the primary stopes are excavated and backfilled, the mine operator exploits the secondary stopes. Such a mining sequence can result in stress concentrations and ground control problems. Longitudinal open stoping, Fig. 3, can arguably provide a better control of stress induced problems, as it minimizes the number of pillars left behind. In longitudinal open stoping the full face (width) of the mineralized zone is mined and this dictates the stope width.

In the pre-feasibility and feasibility stages, when geomechanical data are often limited, the design method of choice is the Stability Graph. This empirical method, popularized by Potvin (1988), relies on a variation of the $Q$ rock classification system, Barton et al. (1974). By setting the stress reduction factor (SRF) to 1 it is possible to define a modified, $Q'$. The influence of stress is accounted in the use of the rock stress factor $A$ while further adjustments account for joint orientation with respect to the excavation and a gravity adjustment factor that quantifies the influence of the possible failure mechanisms. This results in a new index of rock mass quality, the stability number $N'$, Eq. 1.

$$N' = Q' \times A \times B \times C, \tag{1}$$

where

$Q'$ is the modified $Q$ Index.
$A$ is the rock stress factor.
$B$ is the joint orientation adjustment factor.
$C$ is the gravity adjustment factor.

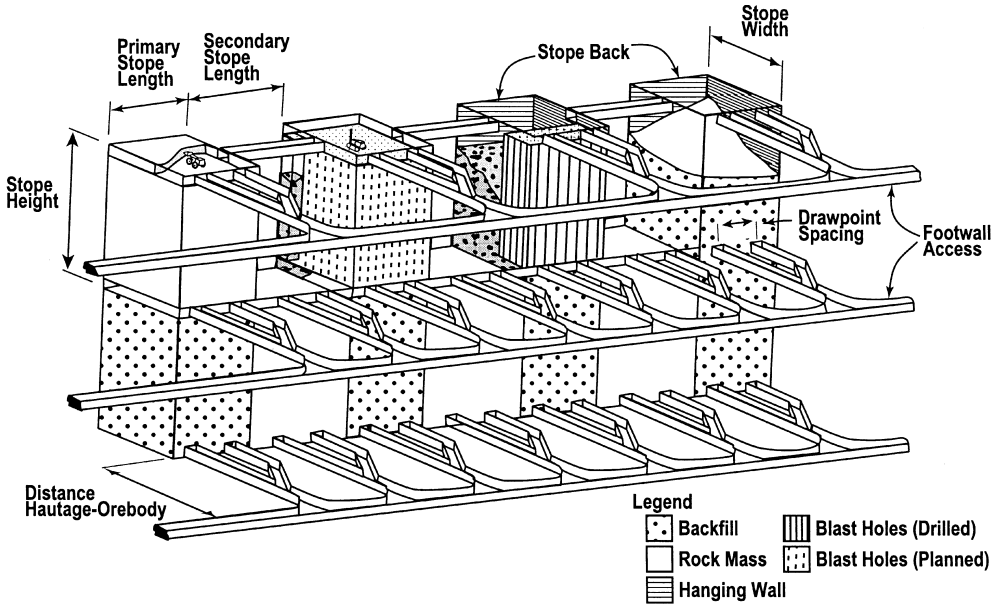


**Fig. 2.** Transversal open stope mining, after Potvin (1988)

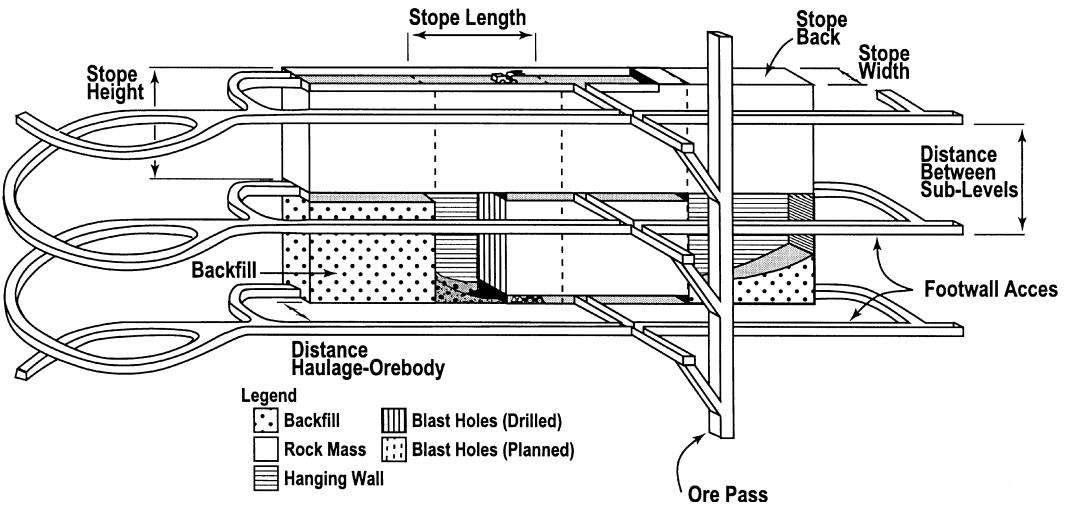


**Fig. 3.** Longitudinal open stope mining, after Potvin (1988)

The stability number ($N'$) is plotted against the hydraulic radius (surface area/perimeter) of the investigated surface (back, hanging wall etc.) of an excavation,

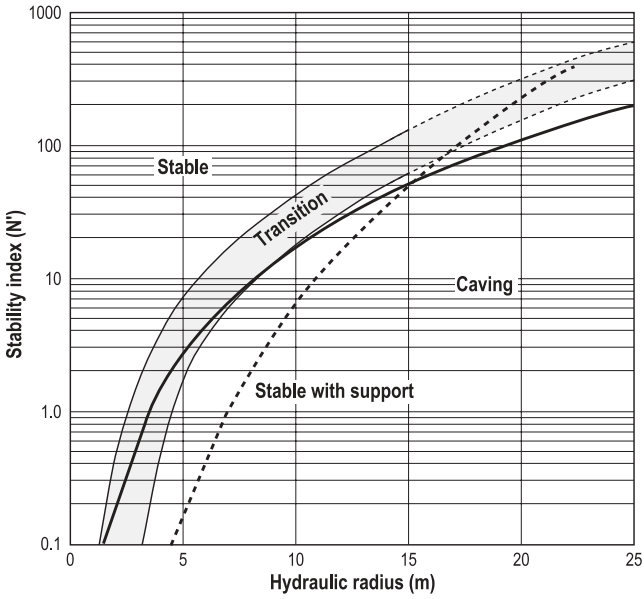


**Fig. 4.** Stability graph design lines after Potvin and Hadjigeorgiou (2001)

Fig. 4. A stope is considered to be stable, in transition or susceptible to caving. Over the years a series of zones of relative stability have been suggested. Potvin and Hadjigeorgiou (2001) provide a full review of the method. Recent modifications have been justified by the use of a larger database of field data. Other adjustments have been proposed to better account for geological complexity, blasting, stress degradation etc. Probabilistic techniques have also received attention to refine the recommendations of the method for different sites as more field data become available.

The success and popularity of the Stability Graph method can be traced to its use as a reliable design tool during the pre-feasibility and feasibility stages, during individual stope planning and for reconciliation analyses. In reviewing the limitation of the method Potvin and Hadjigeorgiou (2001), suggest the Stability Graph is inappropriate in severe rock bursting conditions, in highly deformable rock mass and for entry methods.

Once the mine operation is in development, it is possible to have greater access to the rock exposure. Scanline mapping can then be employed to provide more reliable geomechanical data that can allow for updating the classification results.

At the exploitation stage, numerical methods, and in particular 3D boundary element stress analysis packages, are often employed to determine the more appropriate sequencing. This allows one to better manage the induced stresses and results in improved stability.

In more mature operations, low stress environments are found, in areas where the stresses are shadowed by the presence of other stopes. Under these circumstances, the behavior of a rock mass is influenced by geological structures. Limit

equilibrium methods can then be used to determine the stability of discrete wedges defined by local structural features. A common assumption of most limit equilibrium packages is that all wedges are formed by three joint sets of infinite length.

This paper provides an engineering application of 3D discontinuity networks for a quantitative analysis of the stability of open stopes, where structural features dictate the behavior of the rock mass. The suggested methodology has four distinct steps:

- Geomechanical characterization of the rock mass
- Discontinuity network generation
- Validation of generated discontinuity networks
- Limit equilibrium stability analysis.

Accounting for random joints and using the reported trace lengths results in more realistic wedge representations, with respect to size and their relative position along an excavation. Having identified the wedges it is then possible to incorporate the influence of various rock reinforcement systems (cable bolts, rock bolts and mesh) in any design. Consequently it facilitates the incorporation of risk as an integral part of the design process. This allows one to optimize stope design and support. The logistics of the developed methodology are demonstrated by reference to three documented case studies in a Canadian underground hard rock mine.

## 2. Methodology Overview

Scanline mapping is relatively easy to perform in an underground mine and allows one to adequately sample of the pertinent discontinuity characteristics (position, trace length and orientation). Although, under production constraints, trace length measurements are sometimes ignored at certain mines, they are required input parameters for the developed methodology.

Once the field data are collected, a statistical analysis is performed. Individual joints that are not associated with a particular set are defined as random. It is the authors' experience that these random joints also have an important role in defining the stability of underground excavations.

The disk model developed by Baecher et al. (1977), is used to generate a joint network using the input provided by the statistical analysis. Once a statistical agreement, between in-situ and modeled discontinuity characteristics, is satisfied the generated model is accepted. Although this validation is not absolute, it is far more realistic and rigorous, than the usual characterization techniques currently employed in most underground mines.

Standard limit equilibrium, stability analysis packages are based on somewhat simplistic representation of the rock mass (limited number of joint sets, infinite trace length, etc.). The developed approach overcomes these limitations by introducing the actual geometry and dimensions of any excavation into the simulated 3D joint network. Distinct rock blocks are then created along any excavation surface by the intersection of all generated joint sets, including random joints. The volume, base area and apex length for every block is calculated. With this, one can better account for the inherent rock mass complexity, as well as the influence of

excavation shape and size with regard to structural features. In the three case studies, the interdependence of the excavation span and discontinuity length, and to a lesser degree discontinuity spacing, in defining the blocks size will be evident.

The stability of every individual rock block present along an excavation surface is quantified by a safety factor distribution. Consequently, it is possible to compare the performance of different reinforcement systems in stabilizing the rock mass. This can consider the type of reinforcement (rockbolts, cable bolts, etc.) but also selected configurations (length, patterns). Analyzing safety factor distributions for different reinforcement options results in a rational design that can be extended to include cost analysis.

## 3. Case Studies

The developed methodology is best illustrated by three case studies in an underground mine in Northwestern Quebec, Canada. The Louvicourt mine, Fig. 5, is a polymetallic orebody of copper, zinc, silver and gold. This volcanogenic massive sulfide deposit lies at a depth of 475 m from the surface, and is part of the Abitibi Greenstone belt within the Precambrian shield of Eastern Canada. The mine

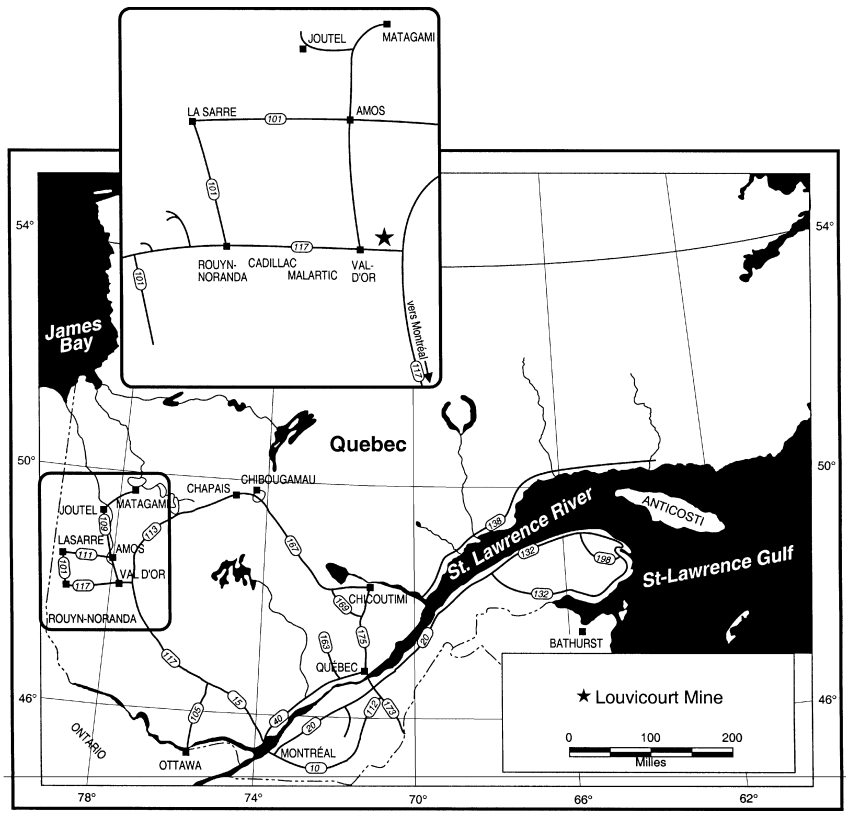


**Fig. 5.** Localisation of Louvicourt Mine

employs transverse blasthole open stopes, 50 m in length, 15 m in width and 30 m in height. Paste backfill is also employed. A preliminary 3D-Joint network analysis for this site has been presented in earlier work by the authors, Grenon and Hadjigeorgiou (2000).

### *3.1 3D Joint Network Modeling*

The influence of geological structure on the stability of underground excavations has never been questioned. The main problematic issues have been our ability to accurately quantify structure and its relative importance to the stability of an excavation. Despite efforts to improve data collection the most reliable technique remains traditional scanline mapping. While the use of empirical classification systems to express this structural complexity has served the mining industry well in the past, it can be argued that the use of a singular rock classification index underutilizes available data, and can fail to capture the inherent structural complexity.

3D joint networks provide an attractive alternative to simulate the natural complexity of a rock mass. Dershowitz and Einstein (1988) provide an excellent review of several geometric models. The more sophisticated geometric models focus on understanding and simulating flow through jointed rock (Dershowitz (1996), Wang et al. (2000) and several others). Ivanova (1998) has contributed to the development of a sophisticated geometric-mechanical model that allows one to account for the prevalent geologic mechanisms.

Prior to selecting a representative 3D joint network for engineering design, it is necessary to define the objective of the analysis and the required degree of accuracy. In investigating the stability of underground mining excavations it is necessary to account both for limited available data as well as operational constraints. In this context the authors have developed a relatively simple, but easy to use, model, Stereoblock. The model is based on the original work of Baecher et al. (1977) whereby joints are represented by disks. Over the years Stereoblock has been modified to include the works of Villaescusa (1991), Lessard (1996), Grenon (2000) and others. In its present form, Stereoblock can simulate any number of joints in any generated volume with computer memory as the only limiting factor. Useful features include using joints of finite size, as well as accounting for random joints.

#### 3.1.1 Structural Data Collection and Analysis

Scanline mapping was used to record orientation, position and trace length of discontinuities for three sites in an underground hard rock mine. The main discontinuity sets were then identified, Fig. 6. For every set its mean orientation and the Fisher coefficient of dispersion (K) (a measure of the dispersion of the poles around the mean value), were calculated. Tables 1 to 3 report the mean normal spacing, mean trace length and the standard deviation for each discontinuity set. Three to four discontinuity sets were identified for every site. Random joints represent 31% of all recorded joints. In an effort to quantify the influence of random joints their spacing and mean trace length were evaluated. Joint censoring was not

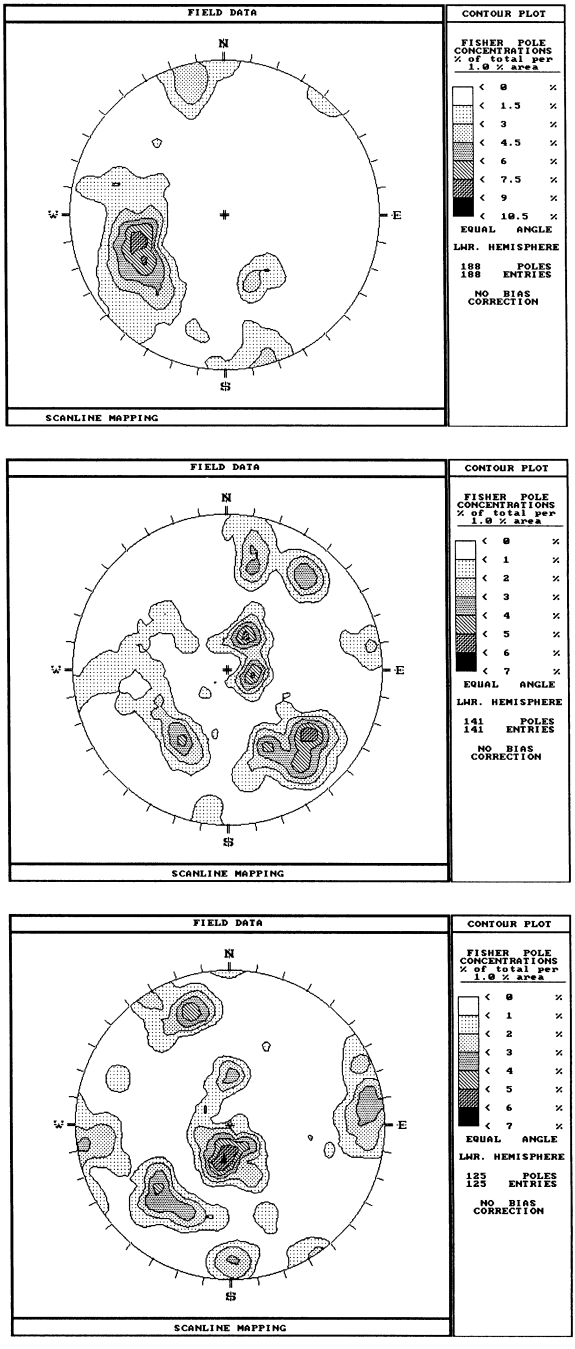


**Fig. 6.** Lower hemisphere stereoplots for the three sites

**Table 1.** Statistical analysis of the first mapped discontinuity network

| | Orientation (°) | K | Average trace length (m) | Trace length standard dev. (m) | Normal spacing (m) |
|---|---|---|---|---|---|
| Set 1 | 61/037 | 13 | 1.40 | 1.30 | 0.23 |
| Set 2 | 49/301 | 69 | 1.00 | 1.10 | 0.71 |
| Set 3 | 90/136 | 43 | 0.83 | 0.91 | 1.00 |
| Random | – | – | 1.00 | 0.90 | 0.91 |

**Table 2.** Statistical analysis of the second mapped discontinuity network

| | Orientation (°) | K | Average trace length (m) | Trace length standard dev. (m) | Normal spacing (m) |
|---|---|---|---|---|---|
| Set 1 | 73/174 | 31 | 1.60 | 0.97 | 0.20 |
| Set 2 | 56/008 | 28 | 0.74 | 0.83 | 0.29 |
| Set 3 | 65/296 | 21 | 1.40 | 1.30 | 0.55 |
| Set 4 | 20/205 | 22 | 0.70 | 0.62 | 0.47 |
| Random | – | – | 0.76 | 0.96 | 1.59 |

**Table 3.** Statistical analysis of the third mapped discontinuity network

| | Orientation (°) | K | Average trace length (m) | Trace length standard dev. (m) | Normal spacing (m) |
|---|---|---|---|---|---|
| Set 1 | 22/238 | 26 | 1.20 | 1.20 | 0.34 |
| Set 2 | 64/009 | 29 | 1.00 | 0.90 | 0.43 |
| Set 3 | 76/128 | 47 | 1.50 | 1.20 | 1.20 |
| Set 4 | 90/234 | 26 | 1.50 | 1.50 | 0.56 |
| Random | – | – | 1.70 | 2.00 | 0.63 |

considered at these sites, as more than 97% of the joints had a length inferior to 3.5 m. Low persistence and moderate to wide spacing (0.20 to 1.60 m) characterize the joint sets.

### 3.1.2 Applicability of Stereoblock

Once the stereonets and data files were introduced into Stereoblock, a statistical analysis defined the distributive nature of orientation, spacing and trace length for every joint set. The in situ discontinuity characteristics, for the three sites, are summarized in Tables 4 to 6. For every discontinuity set parameter a theoretical distribution was tested against the collected data using a $\chi^2$ test. Use of the Fisher univariate distribution to model the orientation dispersion of the pole around the mean value was justified on the basis that ten out of the eleven Fisher distributions tested were accepted. Thirteen out of fourteen spacing distributions were exponen-

**Table 4.** Analysis for site #1

| | Parameter | Distribution | Number of classes | $\chi^2$ test | Accepted |
|---|---|---|---|---|---|
| Set 1 | orientation | Fisher univariate | 7 | 11.02 | yes |
| | spacing | exponential negative | 7 | 0.82 | yes |
| | trace | lognormal | 8 | 16.50 | no |
| Set 2 | orientation | Fisher univariate | 5 | 1.18 | yes |
| | spacing | exponential negative | 6 | 7.21 | yes |
| | trace | lognormal | 7 | 11.84 | yes |
| Set 3 | orientation | Fisher univariate | 5 | 6.55 | yes |
| | spacing | exponential negative | 5 | 2.45 | yes |
| | trace | lognormal | 8 | 7.22 | yes |
| Random | spacing | exponential negative | 6 | 4.60 | yes |
| | trace | lognormal | 6 | 10.59 | yes |

**Table 5.** Analysis for site #2

| | Parameter | Distribution | Number of classes | $\chi^2$ test | Accepted |
|---|---|---|---|---|---|
| Set 1 | orientation | Fisher univariate | 6 | 0.87 | yes |
| | spacing | exponential negative | 7 | 1.06 | yes |
| | trace | lognormal | 7 | 5.42 | yes |
| Set 2 | orientation | Fisher univariate | 6 | 7.81 | yes |
| | spacing | exponential negative | 5 | 4.11 | yes |
| | trace | lognormal | 8 | 6.06 | yes |
| Set 3 | orientation | Fisher univariate | 8 | 5.92 | yes |
| | spacing | exponential negative | 6 | 0.30 | yes |
| | trace | lognormal | 8 | 2.53 | yes |
| Set 4 | orientation | Fisher univariate | 8 | 4.49 | yes |
| | spacing | exponential negative | 6 | 8.20 | yes |
| | trace | lognormal | 6 | 1.41 | yes |
| Random | spacing | exponential negative | 6 | 2.45 | yes |
| | trace | lognormal | 6 | 11.10 | yes |

**Table 6.** Analysis for site #3

| | Parameter | Distribution | Number of classes | $\chi^2$ test | Accepted |
|---|---|---|---|---|---|
| Set 1 | orientation | Fisher univariate | 5 | 29.12 | no |
| | spacing | exponential negative | 5 | 0.95 | yes |
| | trace | lognormal | 5 | 2.75 | yes |
| Set 2 | orientation | Fisher univariate | 8 | 1.65 | yes |
| | spacing | exponential negative | 5 | 16.00 | no |
| | trace | lognormal | 8 | 7.41 | yes |
| Set 3 | orientation | Fisher univariate | 7 | 8.61 | yes |
| | spacing | exponential negative | 5 | 5.10 | yes |
| | trace | lognormal | 5 | 8.72 | yes |
| Set 4 | orientation | Fisher univariate | 5 | 2.45 | yes |
| | spacing | exponential negative | 6 | 4.47 | yes |
| | trace | lognormal | 5 | 5.21 | yes |
| Random | spacing | exponential negative | 6 | 4.17 | yes |
| | trace | lognormal | 7 | 16.80 | no |

tially distributed supporting the case that the discontinuities are randomly distributed in space. Given that twelve out of fourteen of the trace distributions are lognormal it was possible to use the techniques of Villaescusa (1990) to determine the diameter of discontinuities. As a result of the above the use of Stereoblock for the three investigated sites was judged appropriate.

### 3.1.3 Generation of 3D Joint Networks

Having justified the applicability of Stereoblock, a series of 3D models were generated. In the models the discontinuity centers were randomly positioned in three-dimensional space and joint dimensions obtained based on the theoretical development by Waburton (1980), Chan (1986) and Villaescusa (1990). Determination of discontinuity diameters is based on the distributive nature of the trace lengths. For a log normal distribution of joint diameters the following equations are used to evaluate the mean diameter ($\mu_d$) and the standard deviation ($\sigma_d$). For every generated joint, a diameter value is randomly chosen from the diameter distribution described by these two parameters

$$\mu_d = 2\ln E(x) - \frac{1}{2}\ln E(x^2) \tag{2}$$

$$\sigma_d = \ln E(x^2) - 2\ln E(x), \tag{3}$$

where

$$E(x) = \frac{\left[\frac{3\pi\mu_1}{8}\right]^5}{\left[\frac{4}{3}\{\mu_1^2 + \sigma_1^2\}\right]^2} \tag{4}$$

$$E(x^2) = \frac{\left[\frac{3\pi\mu_1}{8}\right]^8}{\left[\frac{4}{3}\{\mu_1^2 + \sigma_1^2\}\right]^3}, \tag{5}$$

where

$\mu_1$ is the mean trace length of a set.
$\sigma_1$ is the standard deviation of the traces of a set.

The volumetric intensity of the discontinuity network was modeled through a procedure suggested by Priest (1993) using virtual scanlines in the simulated network. Joints are generated along these scanlines until the spatial frequency of the generated joints equals the joint frequency recorded during in-situ mapping.

Joint set orientation, spacing and trace length distributions were used to generate a 3-D joint network for a simulated rock volume of $35 \times 35 \times 60$ m. To avoid boundary effects all subsequent analyses were based on an internal volume of $30 \times 15 \times 50$ m.

**Table 7.** Validation of the simulated network for site #1

| | Parameter | Distribution | Number of classes | $\chi^2$ test | Accepted |
|---|---|---|---|---|---|
| Set 1 | orientation | Fisher univariate | 5 | 9.50 | yes |
| | spacing | exponential negative | 6 | 1.46 | yes |
| | trace | lognormal | 7 | 6.87 | yes |
| Set 2 | orientation | Fisher univariate | 6 | 15.76 | no |
| | spacing | exponential negative | 5 | 9.24 | yes |
| | trace | lognormal | 6 | 3.69 | yes |
| Set 3 | orientation | Fisher univariate | 6 | 6.57 | yes |
| | spacing | exponential negative | 5 | 1.87 | yes |
| | trace | lognormal | 6 | 1.99 | yes |
| Random | spacing | exponential negative | 5 | 1.74 | yes |
| | trace | lognormal | 5 | 3.07 | yes |

**Table 8.** Validation of the simulated network for site #2

| | Parameter | Distribution | Number of classes | $\chi^2$ test | Accepted |
|---|---|---|---|---|---|
| Set 1 | orientation | Fisher univariate | 7 | 5.86 | yes |
| | spacing | exponential negative | 7 | 3.25 | yes |
| | trace | lognormal | 7 | 11.53 | yes |
| Set 2 | orientation | Fisher univariate | 5 | 6.88 | yes |
| | spacing | exponential negative | 5 | 0.87 | yes |
| | trace | lognormal | 6 | 7.05 | yes |
| Set 3 | orientation | Fisher univariate | 6 | 3.76 | yes |
| | spacing | exponential negative | 5 | 3.40 | yes |
| | trace | lognormal | 8 | 19.32 | no |
| Set 4 | orientation | Fisher univariate | 6 | 35.66 | no |
| | spacing | exponential negative | 5 | 1.04 | yes |
| | trace | lognormal | 8 | 4.83 | yes |
| Random | spacing | exponential negative | 8 | 7.06 | yes |
| | trace | lognormal | 8 | 11.35 | yes |

#### 3.1.4 Validation

An important element of the developed procedure is validation. Scanline surveys were conducted with the simulated networks, the distributive nature of the various structural parameters defining a discontinuity set were compared to the properties of the input data. The validity of the simulations was supported by a $\chi^2$ test.

Referring to Tables 7 to 9, it can be shown that using a $\chi^2$ test the three generated networks fit the observed distributions for the in-situ data where 34 out of 39 distributions were statistically equivalent. It can be argued that more sophisticated validation approaches might be appropriate. Nevertheless given the problem constraints and the engineering approach used, the $\chi^2$ test was sufficient.

### *3.2 Stability Analysis*

A rock mass is defined by intersecting discontinuities that can contribute to the creation of distinct rock blocks at the periphery of a stope. The presence of such

**Table 9.** Validation of the simulated network for site #3

| | Parameter | Distribution | Number of classes | $\chi^2$ test | Accepted |
|---|---|---|---|---|---|
| Set 1 | orientation | Fisher univariate | 6 | 6.01 | yes |
| | spacing | exponential negative | 5 | 2.16 | yes |
| | trace | lognormal | 8 | 8.77 | yes |
| Set 2 | orientation | Fisher univariate | 6 | 10.61 | yes |
| | spacing | exponential negative | 5 | 3.45 | yes |
| | trace | lognormal | 7 | 6.36 | yes |
| Set 3 | orientation | Fisher univariate | 5 | 1.35 | yes |
| | spacing | exponential negative | 6 | 3.37 | yes |
| | trace | lognormal | 6 | 10.72 | yes |
| Set 4 | orientation | Fisher univariate | 7 | 4.69 | yes |
| | spacing | exponential negative | 7 | 8.18 | yes |
| | trace | lognormal | 6 | 31.15 | no |
| Random | spacing | exponential negative | 8 | 18.87 | no |
| | trace | lognormal | 5 | 6.88 | yes |

wedges can be a main source of structural instability. Consequently, any analysis should be aimed at predicting the risk and cost of a structural failure and the suitability and applicability of any reinforcement system.

Traditional reinforcement analysis and design tools often rely on rock classification systems to provide a unique stability index for the investigated surface (stope back, hanging wall). The limitations of such systems to fully capture the structural regime of a rock mass have been demonstrated by Hadjigeorgiou et al. (1998). Limit equilibrium analyses often rely on three intersecting discontinuities of infinite length to define a potential wedge (Hoek and Brown, 1980). They do not, however, provide any mechanism to identify the critical discontinuities, nor the number and location of possible wedges along a given stope surface.

Esterhuizen and Ackermann (1998) provide an interesting alternative in analyzing the stability of a stope in jointed rock. Monte-Carlo simulations were used to generate a series of typical blocks randomly positioned over a stope surface. A series of checks were conducted in order to assess the efficiency of a given reinforcement pattern and to determine whether a bolt could support a block. Subsequently, it was verified that the investigated block was within the support limit of two adjacent bolts. Following several thousand simulations they assessed the probability of failure for a given excavation. Although this approach is an improvement over empirical efforts, it is limited by the assumed spatial distribution of the blocks, as well as by the assumption that joints are of infinite length. Furthermore, this approach ignores the presence of random joints that can result in a larger number of blocks.

### 3.2.1 Structural Analysis with Stereoblock

Once a 3D joint network is simulated using Stereoblock, it is possible to introduce any form, size and shape of an open stope and investigate its stability. It is then possible to quantify all blocks formed at the periphery of the excavation. Figure 7 is a simplified representation of a section along an investigated stope wall, devel-

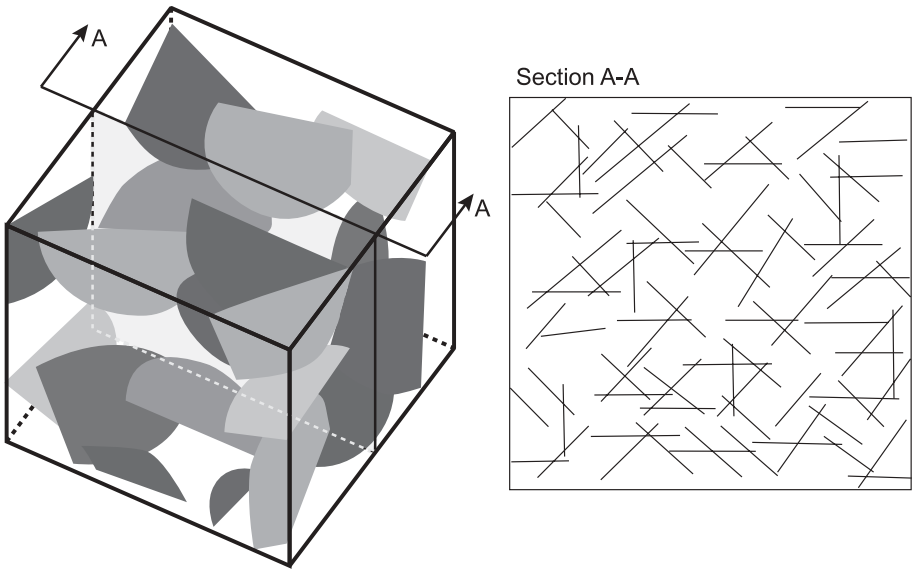


**Fig. 7.** Section cut through the simulated joint network

oped in the simulated network. All intersecting discontinuities are clearly identifiable.

For the encountered conditions, the strength of discontinuities was described by the Coulomb failure criterion. Based on the results of direct shear tests the angle of friction was defined with a mean of 30° and a standard deviation of 2.5° and a mean cohesion value of 300 kN with a standard deviation of 50 kN. Subsequently, for all generated discontinuities the mechanical properties were randomly selected over these normal distributions.

As the geometrical properties are known for all intersected discontinuities it is relatively easy to identify all tetrahedral blocks formed along the investigated section. It is the authors' experience that tetrahedral blocks are the most common type observed in the field. This is supported by independent observations by Windsor (1999). If during the geological mapping a major discrete feature, such as fault, is observed, it is possible to introduce this feature in the 3D model. This opens various possibilities in investigating the potential contributions to the stability of excavation of major structural features.

Figure 8 provides a conceptual view of how blocks of different size can form at the back of a stope. The base area, apex length and volume are determined for every generated rock blocks. Apex length is the perpendicular distance between the base of a block (delimited by the three summits located at back or the wall of a stope) and the peak of the block. For any stope surface it is possible to determine the resulting distributions for every block property. It is also possible to identify the discontinuities involved in the creation of the blocks, enabling one to determine critical sets for a given stope geometry and orientation.

The stability of every individual block is evaluated through the limit equilib-

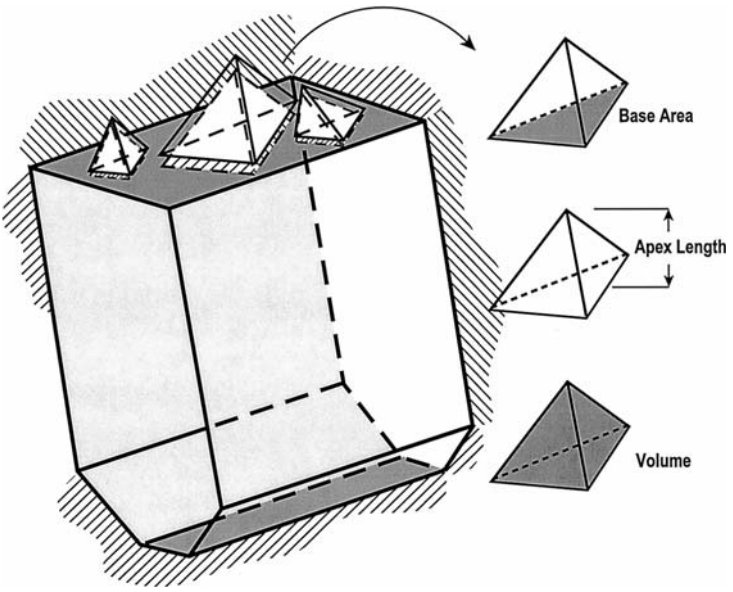


**Fig. 8.** Schematic representation of wedges formed at the back of a stope

rium approach described in Hoek and Brown (1980). This facilitates the determination of an individual safety factor for every block and the associated risk for any given stope size and orientation. The impact of spot or pattern reinforcement is analyzed based on the methodology developed by Li (1991). Figure 9 illustrates the three possible mechanisms for block failure: a) gravity, b) single plane sliding and c) wedge sliding along the line of intersection of two planes. The factor of safety is evaluated according to Eq. 6 to 8.

a) Wedge free to fall from the roof of an excavation

$$FS = \frac{\sum_{l=1}^{n} T_g^l}{W_g}. \tag{6}$$

b) Sliding along a single plane

$$FS = \frac{N_i \cdot tg(\phi_i) + A_i \cdot c_i}{S_i} + \frac{\sum_{l=1}^{n}[(T_{ni}^l \cdot tg(\phi_i) + T_{si}^l)]}{S_i}. \tag{7}$$

c) Wedge sliding along the line of intersection of two planes

$$FS = \frac{N_i \cdot tg(\phi_i) + N_j \cdot tg(\phi_j) + A_i \cdot c_i + A_j \cdot c_j}{S_{ij}} + \frac{\sum_{l=1}^{n}[(T_{ni}^l \cdot tg(\phi_i) + T_{nj}^l \cdot tg(\phi_j) + T_{sij}^l)]}{S_{ij}}; \tag{8}$$

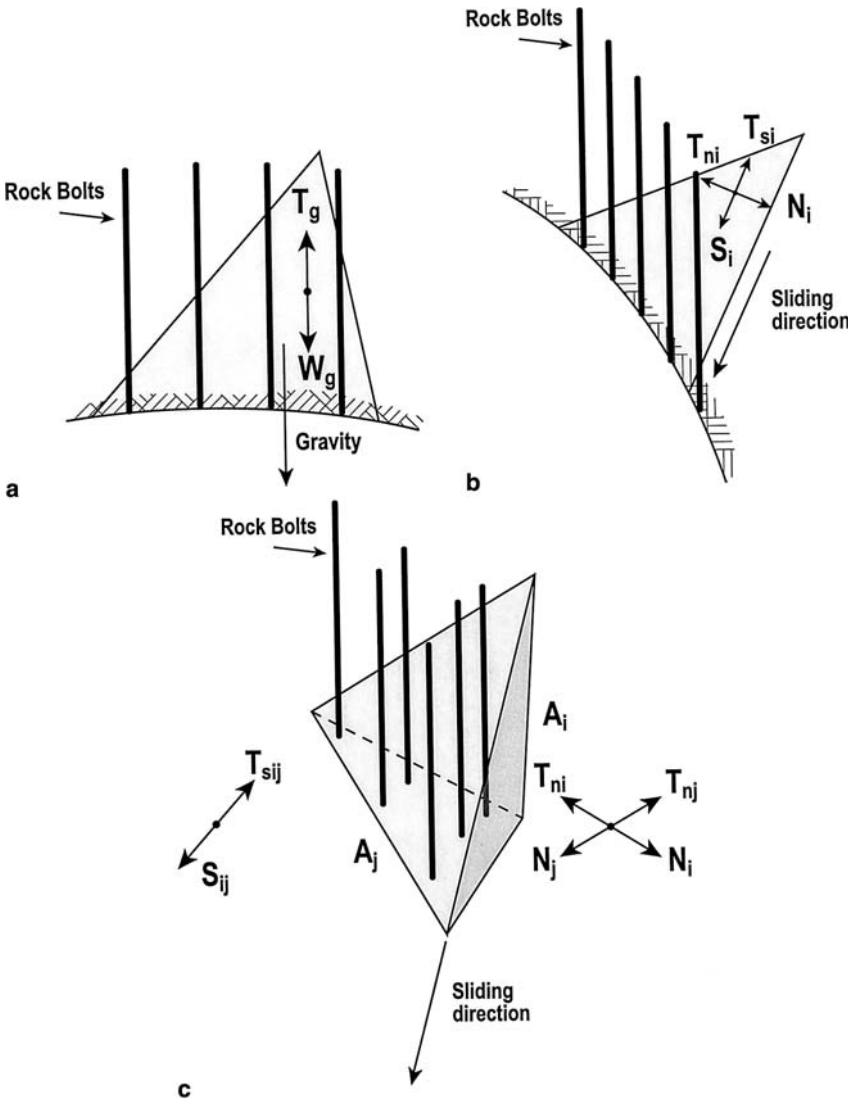


**Fig. 9a–c.** The three possible mechanisms for block failure: **a** gravity, **b** single plane sliding and **c** wedge sliding along the line of intersection of two planes

where

$n$ is the number of bolts.
$W_g$ is the weight in the direction of gravity.
$N_i$ is the proportion of the block's weight normal to plane $(i)$.
$S_i$ is the proportion of the block's weight tangential to plane $(i)$ in the direction of sliding.
$S_{ij}$ is the proportion of the block's weight in the direction of the intersection line between plane $i$ and $j$.
$T_g$ is the component of the bolt capacity $(T)$ in direction of gravity.

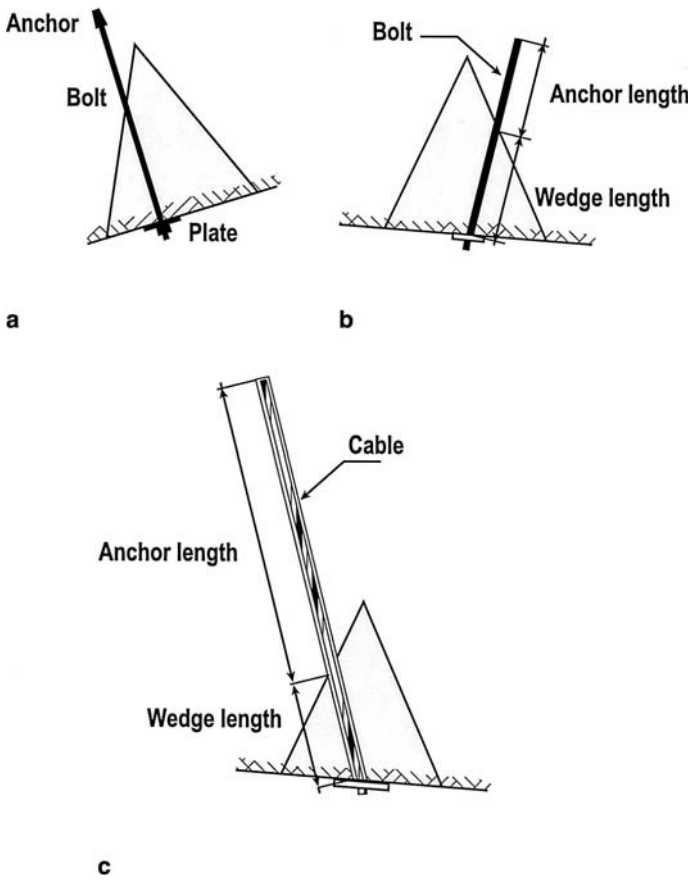


**Fig. 10a–c.** Different type of bolts: **a** mechanically anchored bolt, **b** frictional bolt and **c** grouted bolt or cable

$T_{ni}$ is the component of the bolt capacity $(T)$ normal to plane $(i)$.
$T_{si}$ is the component of the bolt capacity $(T)$ tangential to plane $(i)$ and in the sliding direction.
$T_{sij}$ is the component of the bolt capacity $(T)$ in the direction of the line of intersection of plane $i$ and $j$.
$A_i$ is the area of plane $(i)$.
$c_i$ is the cohesion of plane $(i)$.
$\varphi_i$ is the friction angle of plane $(i)$.

At the design stage this approach can be used to compare different reinforcement strategies. Li's model can account for different type of rockbolts and cablebolts, Fig. 10. The capacity of mechanical bolts is based on the weakest link basis from the rockbolt, plate or shell. In the use of fully grouted bolts/cables or frictional bolts it is the steel capacity, the frictional or bounding strength over the anchor or the wedge length that is the weakest link. The final engineering design is based both on technical and economic concerns.

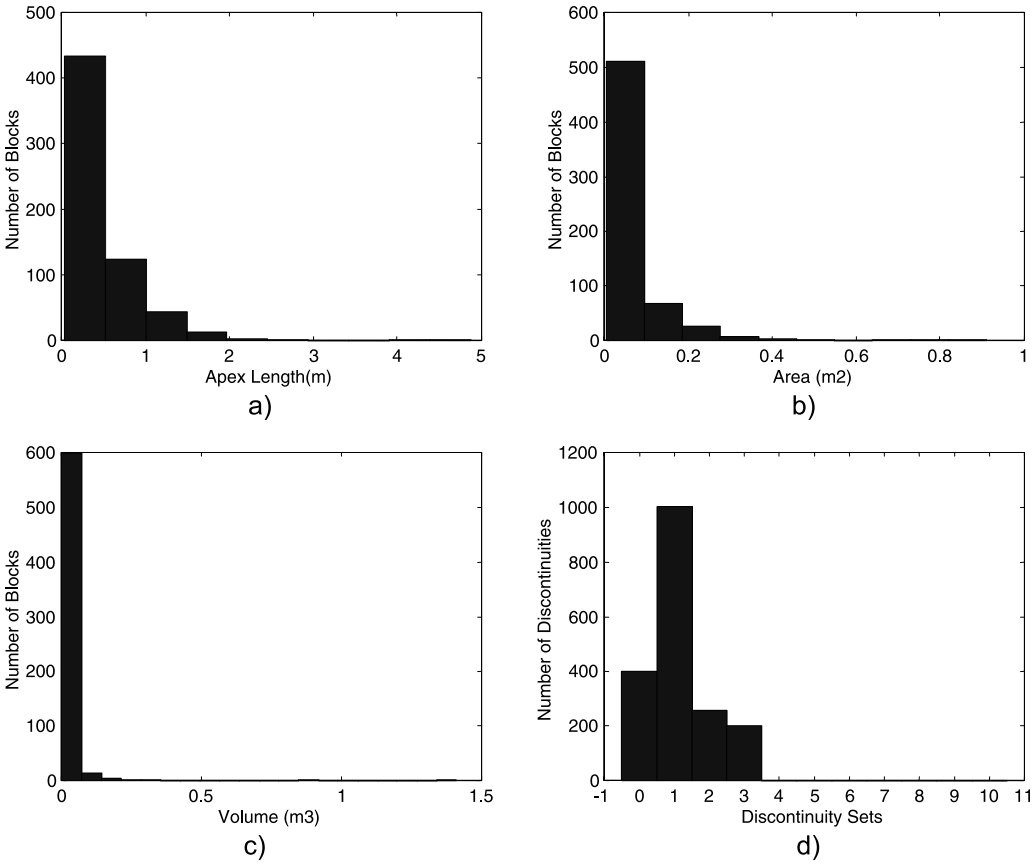


**Fig. 11.** Quantification of the geometrical distributions for site #1: **a** Number of blocks versus apex length, **b** number of blocks versus base area, **c** number of blocks versus volume, **d** number of discontinuities per set

### 3.2.2 Results of the Stability Analysis

Once the discontinuity networks were generated and validated, all blocks formed at the stope backs were characterized based on their geometric properties. The kinematic stability of every block was calculated as the influence of the employed reinforcement at these sites. For the investigated stope backs of 50 m by 15 m, the mine used a standard reinforcement pattern of:

- 10 m cables on a $2 \times 2$ m pattern.
- 2.1 m grouted rebars on a $1.2 \times 1.2$ m pattern.
- Gage 9 welded mesh.

#### *3.2.2.1 Stope #1 results*

Based on the undertaken simulations the geometric properties of all blocks intersecting the stope back for stope #1 are presented in Fig. 11. A total of 621 blocks

were created at the back of the stope. A closer inspection reveals that the majority of blocks are relatively small in size. In fact, very few blocks have an apex length exceeding 3 m and no block has a volume greater than 0.5 $m^3$. The importance of introducing random discontinuities is demonstrated in Fig. 11d. Some 400 random discontinuities (set 0) contribute in defining rock blocks. In other words, more than 22% of all created blocks had at least one surface belonging to a random discontinuity.

The results of the stability and reinforcement analysis are presented in Fig. 12. In Fig. 12a the distribution of the safety factors for each block intersecting the stope back is noted while 12b demonstrates the impact of the standard reinforcement pattern used by the mine. It is important to point out that the use of reinforcement results in several blocks having a considerably higher factor of safety. These blocks were shown to be the larger ones and their corresponding lengths and area distributions are shown in Figs. 12c and 12d. Use of 10 m cables on a $2 \times 2$ m pattern and 2.1 m grouted rebars installed in a $1.2 \times 1.2$ m patterns intersected the bigger blocks and provided the necessary support. It is evident, however, that in the investigated case study the use of reinforcement has minimal impact on the safety factor distribution. Of interest was the large number of smaller blocks. These are due to the fact that at this particular site the joint trace lengths were small. The smallest blocks are expected to fall during the blasting. Based on the results of Tannant (1995) it was possible to determine the capacity of mesh that could be used to support the smaller blocks. When type 9 mesh is used with a 1.2 by 1.2 m bolt pattern, the mesh can sustain blocks having a weight up to 1.5 t. In the present case all generated blocks weighted less than 1.5 t. Thus, a support system using mesh, cables and bolts was more than adequate to support all the created blocks.

A further necessary condition for reinforcement is that the length of any reinforcement unit is long enough to anchor any block into the stable rock. Based on the block apex length dimensions the cable lengths were long enough to reinforce 100% of the blocks while the rebar length was sufficient to stabilize 98% of them. Figure 12e shows the number of bolts that intercept a rock block where out of the 746 reinforcement units installed, only 90 intercepted a rock block. This would suggest that only 12% of the reinforcement units are active at this site.

#### *3.2.2.2 Stope #2 results*

Given that stope #2 had the same dimensions and reinforcement system as stope #1, the same volume of simulated discontinuity networks was employed. The results of the simulations are shown in Fig. 13. At the back of the stope 1393 blocks were created with majority of those being quite small, Figs. 13a to 13c. Joint sets one and three were the most critical in defining blocks intersecting the back of the excavation. The safety factor distribution for the case without reinforcement, is presented in Fig. 14a, where only 11% of the blocks are stable. Figure 14b shows that bolting results in 22% of the blocks being adequately reinforced and the use of screen allows for full support of the smaller size blocks. The

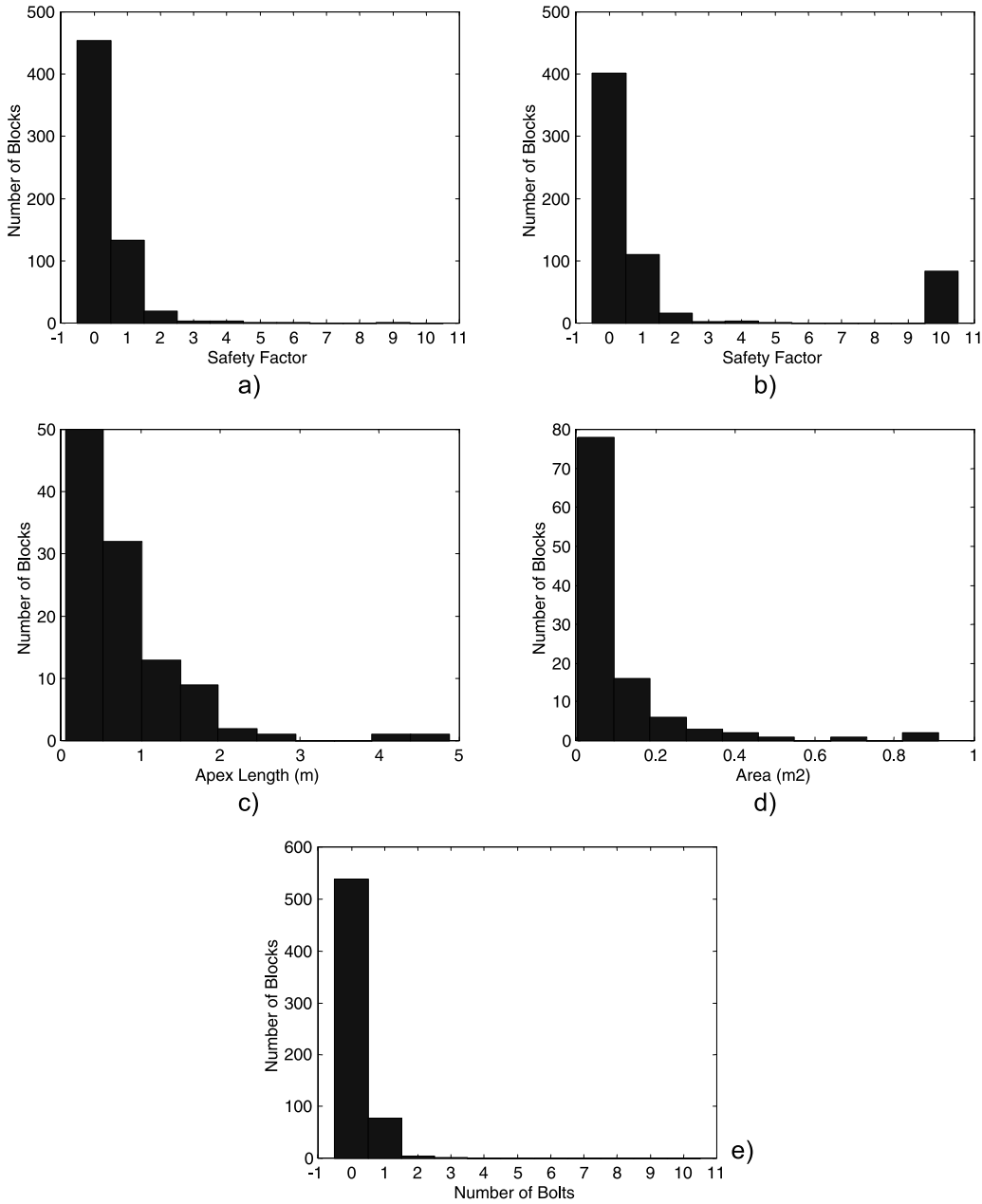


**Fig. 12.** Stability information for site #1: **a** Safety factor distribution (without reinforcement), **b** safety factor distribution (with reinforcement), **c** number of reinforced rock blocks versus apex length, **d** number of reinforced rock blocks versus area, **e** number of blocks intercepted by a bolt

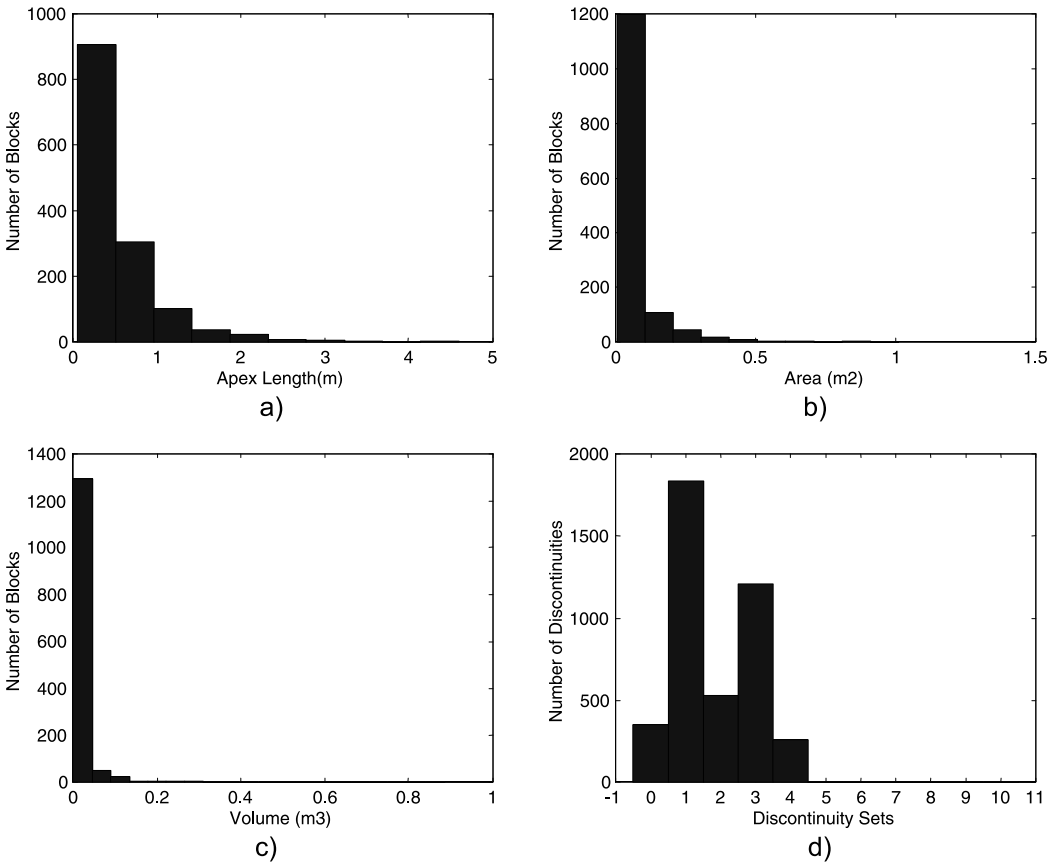


**Fig. 13.** Quantification of the geometrical distributions for site #2: **a** Number of blocks versus apex length, **b** number of blocks versus base area, **c** number of blocks versus volume, **d** number of discontinuities per set

selected combination of cables, rebar and weld mesh was successful in stabilizing the back of the stope.

### *3.2.2.3 Stope #3 results*

Figure 15 presents the results for stope #3 where 1110 blocks were created at the back of the stope. As before these blocks are small in size (Fig. 15a to 15c). As demonstrated on Fig. 15d the large number of rock blocks is due to the presence of random discontinuities, which shows that random discontinuities are critical in defining the created rock blocks. Safety factor distributions are presented in Fig. 16a where 12% of the blocks have a safety factor greater then one. When reinforcement is used, the bolts adequately support 23% of the blocks, Fig. 16b. The weld mesh in itself is able to contain the smaller blocks.

Once the stopes were blasted and mucked, a cavity monitoring system (CMS)

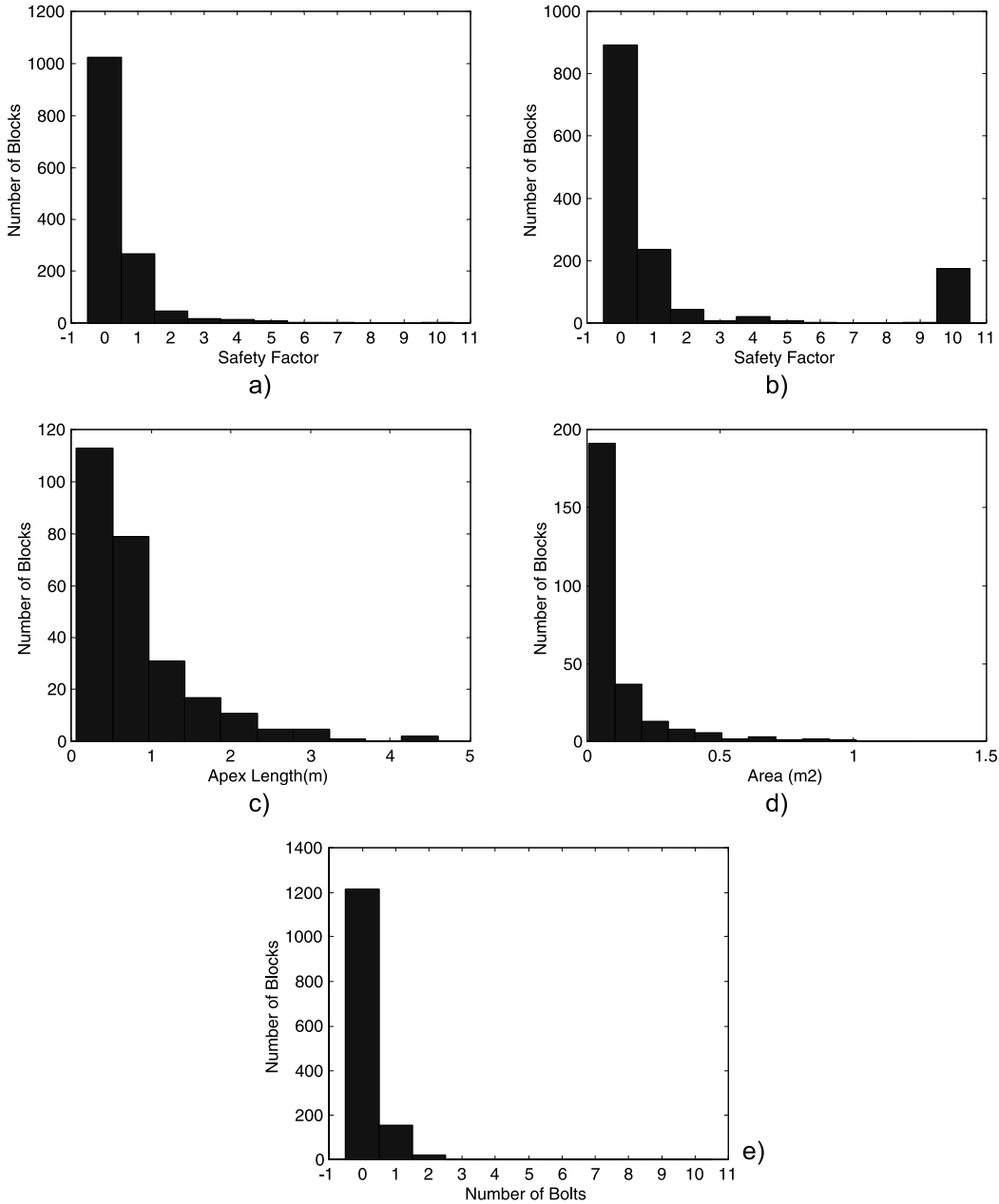


**Fig. 14.** Stability information for site #2: **a** Safety factor distribution (without reinforcement), **b** safety factor distribution (with reinforcement), **c** number of reinforced rock blocks versus apex length, **d** number of reinforced rock blocks versus area, **e** number of blocks intercepted by a bolt

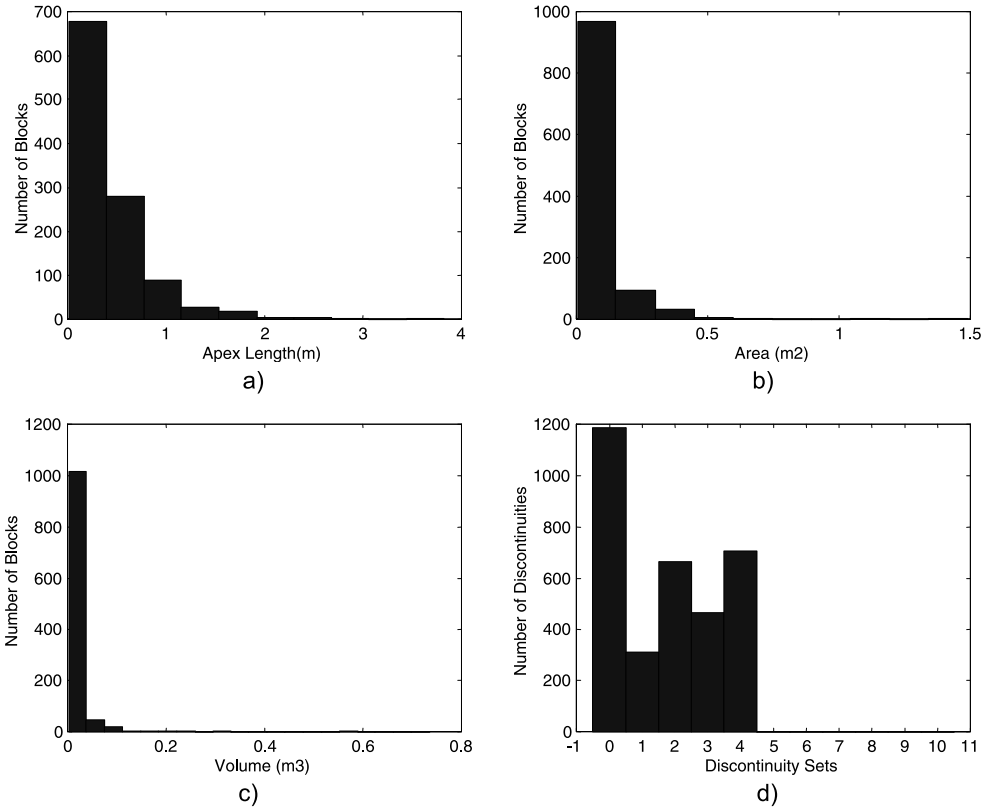


**Fig. 15.** Quantification of the geometric distributions for site #3: **a** Number of blocks versus apex length, **b** number of blocks versus base area, **c** number of blocks versus volume, **d** number of discontinuities per set

was used to quantify the stability of the back and walls. In these particular cases it was shown that the backs remained stable, which is in agreement with the presented analysis.

## 4. Conclusions

This paper has presented an engineering methodology to generate a 3D representation of the discontinuity network based on field data. This has laid the foundation for a more realistic approach to evaluate the stability of rock blocks at the boundary of an underground open stope.

In the three investigated case studies at an underground mine, the method was proven useful to determine the size, probability of occurrence, and stability of the created rock wedges at the back of a stope. It was shown that rock bolts and cable bolts were effective in stabilizing the larger blocks created at the excavation free face.

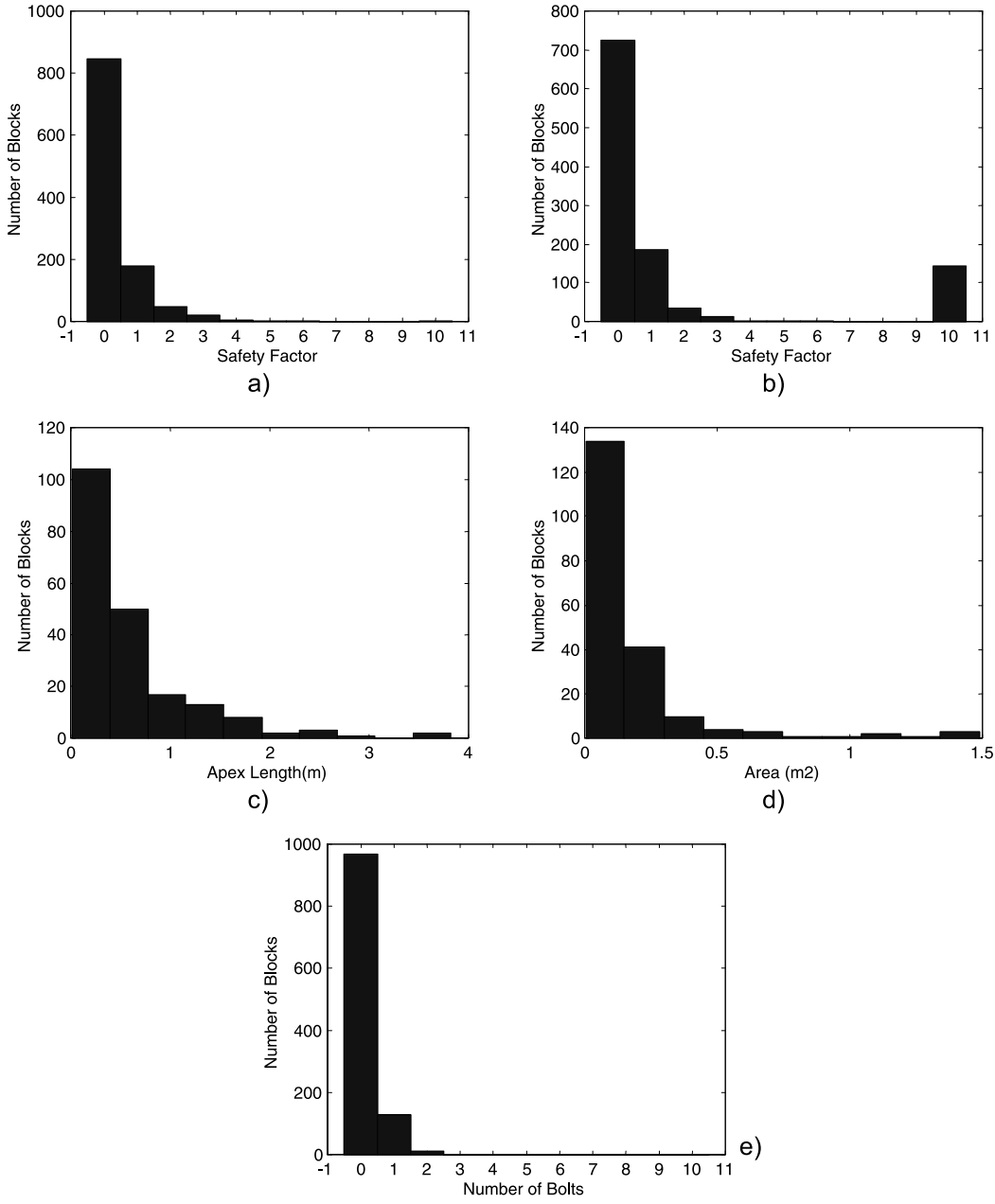


**Fig. 16.** Stability information for site #3: **a** Safety factor distribution (without reinforcement), **b** safety factor distribution (with reinforcement), **c** number of reinforced rock blocks versus apex length, **d** number of reinforced rock blocks versus area, **e** number of blocks intercepted by a bolt

It was further demonstrated that the employed wire mesh adequately retained the smaller blocks. Consequently, the support system employed by the mine, a combination of cables, rebars and mesh was an adequate solution as supported by the results of the cavity monitoring surveys. The groundwork is in place for further simulations that can be performed to investigate the use of other reinforcement systems. Such analysis would help the mining engineer in choosing a reinforcement system giving the same level of safety, but at lower costs.

## Acknowledgments

The financial support of the National Science and Engineering Council of Canada and the Institut de Recherche en Santé et Sécurité au Travail of Quebec and Noranda Inc. is greatly appreciated.

## References

Baecher, G. B., Lanney, N. A., Einstein, H. H. (1977): Statistical description of rock properties and sampling. In: Proc. 18th. U.S. Symp. on Rock Mechanics, Colorado, 5C1.1–5C1.8.

Barton, N. R., Lien, R., Lunde, J. (1974): Engineering classification of rock masses for the design of tunnel support. Rock Mech. 6, 189–239.

Chan, L. P. (1986): Application of block theory and simulation techniques to optimum design of rock excavation. Ph.D. Thesis, University of California, Berkley.

Dershowitz, W. S. (1996): Rock mechanics approaches for understanding flow and transport pathways. Eurock'96, Vol. 3, 1569–1583.

Dershowitz, W. S., Einstein, H. H. (1988): Characterizing rock joint geometry with joint system models. Rock Mech. Rock Engng. 20 (1).

Esterhuizen, G. S., Ackermann, K. A. (1998): Stochastic keyblock analysis for stope support design. Int. J. Rock Mech. Min. Sci. 35 (4–5), Paper no 122.

Grenon, M. (2000): Conception des excavations souterraines à l'aide de la modélisation des réseaux de discontinuités. Ph.D. Thesis, Université Laval.

Grenon, M., Hadjigeorgiou, J. (2000): Stope design based on realistic joint networks. MassMin 2000, 765–771.

Hadjigeorgiou, J., Grenon, M., Lessard, J. F. (1998): Defining in-situ block size. CIM Bull. 91 (1020), 72–75.

Hamrin, H. (2001): Undergound mining methods and applications (2001). In: Hustrulid, W. A., Bullock, R. L. (eds), Underground mining methods: engineering fundamentals and international case studies. Society for Mining, Metallurgy and Exploration, Inc. SME, 3–14.

Hoek, E., Brown, E. T. (1980): Underground excavations in rock. The Institution of Mining and Metallurgy, London.

Hoek, E., Kaiser, P. K., Bawden, W. F. (1995): Support of underground excavations in hard rock. A. A. Balkema, Rotterdam.

Ivanova, V. M. (1998): Geologic and stochastic modeling of fracture systems in rocks. Ph.D. Thesis, MIT, Doston.

Li, B. (1991): The stability of wedges formed by three intersecting discontinuities in the rock surrounding underground excavations. Ph.D. Thesis, University of Toronto.

Lessard, J. F. (1996): Evaluation de la blocométrie des massifs rocheux. Mémoire de Maitrise, Université Laval.

Potvin, Y. (1988): Empirical open stope design in Canada. Ph.D. Thesis, University of British Columbia.

Potvin, Y., Hadjigeorgiou, J. (2001): The stability graph method for open stope design. In: Hustrulid, W. A., Bullock, R. L. (eds), Undergound mining methods: engineering fundamentals and international case studies. Society for Mining Metallurgy and Exploration, Inc. SME, 513–520.

Potvin, Y., Hudyma, M. (2000): Open stope mining in Canada. MassMin 2000, 661–674.

Priest, S. D. (1993): Discontinuity analysis for rock engineering. Chapman & Hall, London.

Tannant, D. (1995): Load capacity and stiffness of welded-wire mesh. 48th Canadian Geotechnical Conference, Vancouver, Canada.

Villaescusa, E. (1991): A three dimensional model of rock jointing. Ph.D. Thesis, University of Queensland.

Warburton, P. M. (1980): A stereographical interpretation of joint trace data. Int. J. Rock Mech. Sci. Geomech. Abstr. 17, 181–190.

Wang, M., Kulatilake, P. S., Panda, B. B. (2000): Discrete fracture fluid flow simulation of pumping tests in a fractured rock. Pacific Rocks 2000. A. A. Balkema, Rotterdam, 831–839.

Windsor, C. R. (1999): Systematic design of reinforcement and support schemes for excavations in jointed rock. In: Proc., International Symposium on Ground Support, Kalgoorlie, Australia. 35–58.

**Authors' address:** Prof. John Hadjigeorgiou, Université Laval, Department of Mining, Metallurgy and Materials Engineering, G1K 7P4 Quebec City, Quebec, Canada; e-mail: john.hadjigeorgiou@gmn.ulaval.ca